

VHE emission in μ Q jets/ISM interactions

Pol Bordas

V. Bosch-Ramon, M. Perucho, J. M. Paredes

Heidelberg, December 2nd 2010



Outline

Outline

- extragalactic \rightarrow galactic ?

Outline

- extragalactic \rightarrow galactic ?
- Interaction model

Outline

- extragalactic \rightarrow galactic ?
- Interaction model
- Hydrodynamical simulations

Outline

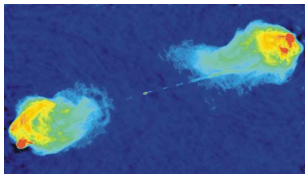
- extragalactic \rightarrow galactic ?
- Interaction model
- Hydrodynamical simulations
- Application to SS433/W50

Outline

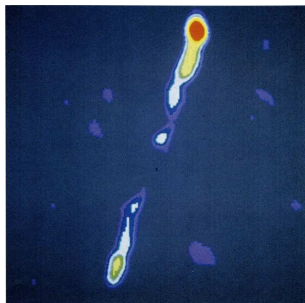
- extragalactic \rightarrow galactic ?
- Interaction model
- Hydrodynamical simulations
- Application to SS433/W50
- Conclusions

Jet-medium interactions

Quasar/IGM interactions \iff μ -quasar/ISM interactions?



Cygnus A
(Perley et al. 1984)



1E 1740
(Mirabel et al. 1992)

FR galaxies and microquasars

similar jet physics...

- Relativistic jets ($l_{\text{jet}} \sim$ light-years in μ -quasars, $l_{\text{jet}} \sim$ mega-light-years in quasars)
- Accretion \rightarrow jet ejection (magnetohydrodynamical?) origin
- Non-thermal radio to γ -ray emission mechanisms
- "Fundamental Plane" $L_{\text{radio}} \propto L_X^{0.6} M_{\text{bh}}^{0.8}$ (phenomenological)

...but some (relative) differences

- Heinz (2002): jet-medium interaction dynamics depend on $\eta = \frac{L_{\text{jet}}}{R^2} \frac{1}{\rho c_s^3}$
- η being M_{bh} -independent $\Rightarrow \rho \propto M_{\text{bh}}^{-1} \Rightarrow \left\{ \begin{array}{ll} \rho \gtrsim 10^4 \text{ cm}^{-3} & \text{and/or} \\ L_{\text{jet}} \text{ much larger} & \text{and/or} \\ L_{\text{jet}} \text{ more powerful} & \text{and/or} \\ F_\nu \text{ much fainter} & \end{array} \right.$

- High-mass systems

SS 433

Cyg X-1

Cyg X-3

LSI 61+303

LS 5039

V4641 Sgr

- Low-mass systems

Cir X-1

XTE J1550-564

1E 1740.7-2942

GRS 1758-258

H 1743-32

Scorpius X-1

GRS 1915+105

GRO J1655-40

GX 339-4

XTE J1748-288

- High-mass systems

SS 433 (Zealey et al. 1980, Dubner et al. 1998)

Cyg X-1 (Martí et al. 1996, Gallo et al. 2005)

Cyg X-3 ? (Heindl et al. 2003, Sánchez-Sutil 2008)

LSI 61+303 ? (Paredes et al. 2007, Rea et al. 2010)

LS 5039

V4641 Sgr

- Low-mass systems

Cir X-1 (Tudose et al. 2006, Heinz et al. 2007)

XTE J1550-564 (Corbel et al. 2002, Kaaret et al. 2003)

1E 1740.7-2942 (Mirabel et al. 1993)

GRS 1758-258 (Martí et al. 2002)

H 1743-32 (Corbel et al. 2005)

Scorpius X-1 (Fomalont et al. 2001)

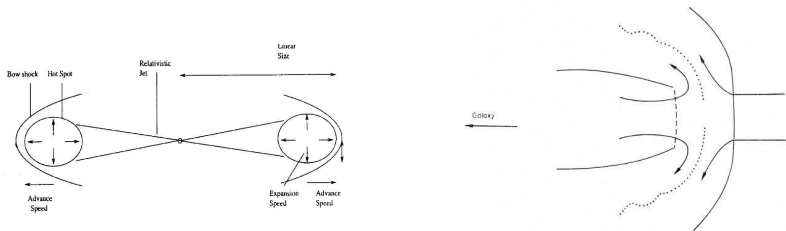
GRS 1915+105 ? (Kaiser et al. 2004, Zdziarski et al. 2005)

GRO J1655-40

GX 339-4

XTE J1748-288

Jet-medium interactions



Extragalactic sources

- Relativistic ($\Gamma \gtrsim 10$), conical + reconfined jets, $l_{jet} \gtrsim 10^{22}$ cm
- Non-thermal “hot spots” and knots (at the reverse shock/recollimation shock?)
- Double radio synchrotron emission lobes
- Stratified environment, $\rho \propto R^{-\alpha} (\alpha \sim 2) \sim 10^{-2} - 10^{-4} \text{ m}_p \text{ cm}^{-3}$;

galactic sources

- Mildly relativistic ($\Gamma \sim 1 - 2$) jets, $l_{jet} \gtrsim 10^{19}$ cm
- Jet's $\theta_{init} = 0.1$ rad + reconfinement at $l_{rec} \sim 10^{18}$ cm
- Interaction zones: reconfinement region, cocoon & shell
- $\rho_{ISM} \sim 0.1 - 1.0 \text{ m}_p \text{ cm}^{-3}$ + companion winds, SNR shell...

Jet-medium interaction model

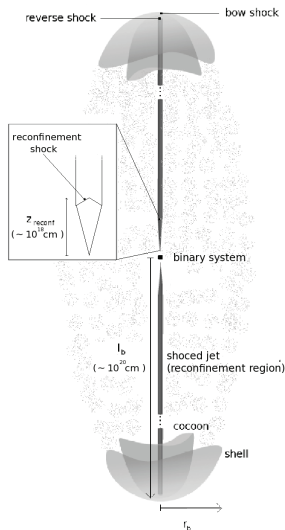
Self-similar growing

- Self-similar parameter: $\mathcal{R} \equiv l_{\text{jet}} / r_{\text{jet}}$
- Source basic parameters:
 - Source age $t_{\mu\text{Q}} \sim 10^4 - 10^5 \text{ yr}$
 - Energy injection rate $Q_{\text{jet}} \sim 10^{36} - 10^{37} \text{ erg s}^{-1}$
 - Medium density $n_{\text{ISM}} = 0.1 - 1.0 \text{ cm}^{-3}$

Characteristic length: $l_0 = \frac{Q_{\text{jet}}^2}{\rho_{\text{ISM}}^2 c^6 (\Gamma_{\text{jet}} - 1)^3}^{1/4}$

given $l_{\text{jet}} \gg l_0$, then

$$\begin{cases} l_{\text{bow}} = 1.5 \left(\frac{Q_{\text{jet}}}{\rho_{\text{ISM}}} \right)^{1/5} t_{\text{MQ}}^{3/5} \\ v_{\text{bow}} = \frac{d}{dt}(l_b) = \frac{3l_b}{5t_{\text{MQ}}} \\ r_{\text{bow}} = l_b / \mathcal{R} \end{cases}$$



Jet-medium interaction model

shock conditions

- Forward shock: $\mathcal{M} = v_{\text{bow}} \cdot \left(\frac{\rho_{\text{ISM}}}{\Gamma_{\text{ISM}} \rho_{\text{ISM}}}\right)^{1/2}$, $\rho_{\text{sh}} = \left(\frac{\Gamma_{\text{ISM}}+1}{\Gamma_{\text{ISM}}-1}\right) \rho_{\text{ISM}}$, $P_{\text{sh}} = \frac{3-(3/5)\mathcal{M}^2}{4} \cdot \rho_{\text{ISM}} v_{\text{bow}}$
- Reverse shock: $\rho_{\text{shocked}} = \left(\frac{\gamma_{\text{ad}} \Gamma_{\text{jet}} + 1}{\gamma_{\text{ad}} - 1}\right) \rho_{\text{rec.jet}}$, $P_{\text{shocked}} = (\gamma_{\text{ad}} - 1)(\Gamma_{\text{jet}} - 1) \cdot \rho_{\text{shocked}} c^2$
- Reconfinement shock: $\rho_{\text{shocked}} = \frac{\Gamma_{\text{jet}} + 1}{\Gamma_{\text{jet}} - 1} \rho_{\text{jet}}(z)$, $P_{\text{shocked}} = P_{\text{cocoon}} \sim \frac{Q_{\text{jet}} t \mu Q}{V_{\text{b}}}$; $V_{\text{b}} \sim (4/3) \pi r_{\text{b}}^2 \times l_{\text{b}}$

non-thermal emitters

- Shell and cocoon: one zone model (B , U_{ph} taken homogeneous); recollimation: $U_{\text{ph}}(z)$
- $\int N_0(E) E dE = \chi Q_{\text{jet}}$; $N_0(E) \propto E^{-p}$; $p = 2.1$
- $u_{\text{B}} = B^2/8\pi = 10\%$ ram/thermal pressure
- Magnetic field equipartition fraction: $B = \eta u_e$ in each interaction zone
- $$U_{\text{phot}} = \begin{cases} \frac{L_{\star}}{4 \pi c l_{\text{bow}}^2}; u_{\text{CMB}} & \text{cocoon \& shell} \\ u(z_{\text{reconf}}) \times \left(\frac{z_{\text{jet}}}{z_{\text{reconf}}}\right)^2; & \text{reconfinement region} \end{cases}$$
- spectral aging of the non-thermal particle populations: $N_0(E) \rightarrow N(E, t)$

Hydrodynamical simulations

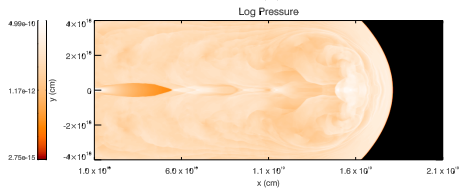
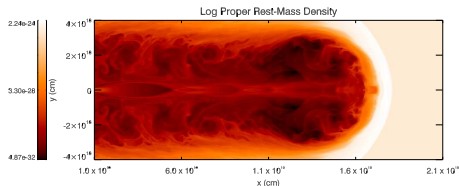
Numerical setup

- two-dimensional finite code to solve the equations of relativistic hydrodynamics (Perucho et al. 2005, 2007)
- axial symmetry, two-dimensional cylindrical coordinates (R, z)
- low resolution \rightarrow macroscopic features only (not mixing nor turbulence studies allowed)
- $t_{\text{evol}} \approx 5 \times 10^4 \text{ yr}$

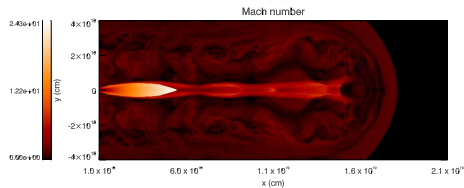
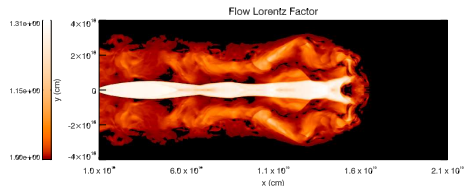
parameter	input value
ambient density	$n_{\text{ext}} = \text{cte} = 0.3 \text{ cm}^{-3}$
initial jet density	$n_{\text{jet}} = 1.4 \times 10^{-5} \text{ cm}^{-3}$
jet power	$L_{\text{jet}} = 3 \times 10^{36} \text{ erg s}^{-1}$
source age	$t_{\text{src}} = 3 \times 10^4 \text{ yr}$
initial jet radius	$r_{\text{jet}} = 2 \times 10^{16} \text{ cm}$
initial jet velocity	$v_{\text{jet}} = 0.6 c$
initial jet Mach number	$\mathcal{M} = 6.5$

Hydrodynamical simulations

$\rho(z, r)$ and $P(z, r)$



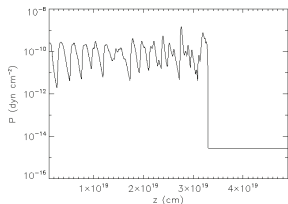
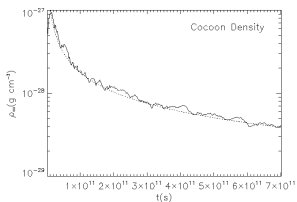
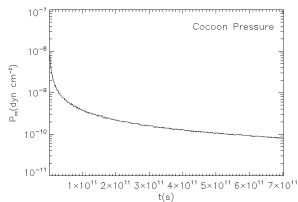
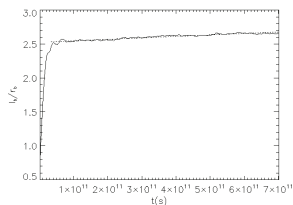
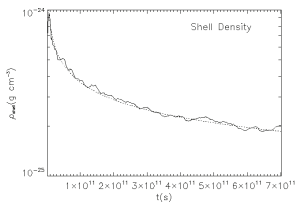
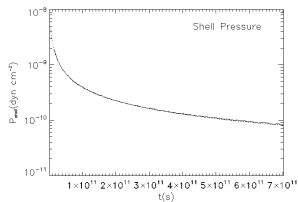
$\Gamma(z, r)$ and $\mathcal{M}(z, r)$



(Bordas et al. 2009)

Hydrodynamical simulations

Pressure and mass densities (shell and cocoon)



hydrodynamical simulations

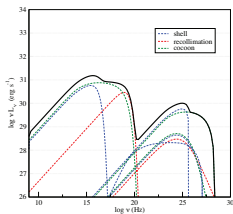
Checking the analytical model

- $l_{\text{bow}} \sim 3.3 \times 10^{19} \text{ cm}$; $v_{\text{bow}} \sim 3 \times 10^7 \text{ cm s}^{-1}$; $\mathcal{R} = 2.7$
- $P_{\text{coc/shell}} \sim 10^{-10} \text{ erg cm}^{-3} \gg P_{\text{ISM}}$
- $\rho_{\text{shell}} \sim 2 \times 10^{-25} \text{ g cm}^{-3}$, $\rho_{\text{coc}} \sim 4 \times 10^{-29} \text{ g cm}^{-3}$
- strong reconfinement shock at $z_{\text{reconf}} \sim 2 \times 10^{18} \text{ cm}$

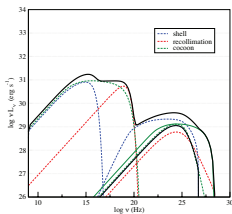
Checking the analytical model

- multiple reconfinement conical shocks after z_{reconf} until $z \lesssim l_{\text{bow}}$
- coupling to a Kelvin-Helmholtz instability?

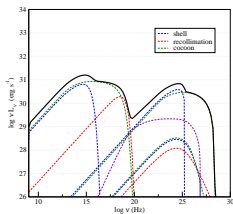
Broadband non-thermal emission



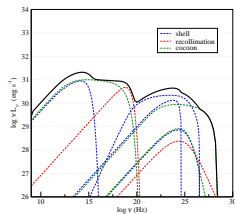
$10^4 \text{ yr}, 10^{36} \text{ erg s}^{-1}, 0.1 \text{ cm}^{-3}$



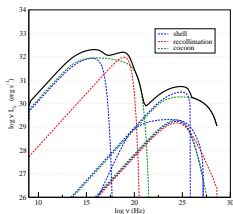
$10^4 \text{ yr}, 10^{36} \text{ erg s}^{-1}, 1.0 \text{ cm}^{-3}$



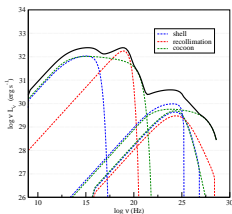
$10^5 \text{ yr}, 10^{36} \text{ erg s}^{-1}, 0.1 \text{ cm}^{-3}$



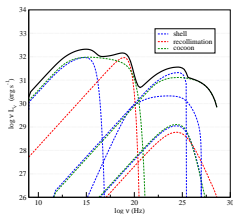
$10^5 \text{ yr}, 10^{36} \text{ erg s}^{-1}, 1.0 \text{ cm}^{-3}$



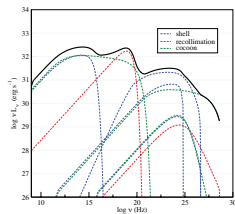
$10^4 \text{ yr}, 10^{37} \text{ erg s}^{-1}, 0.1 \text{ cm}^{-3}$



$10^4 \text{ yr}, 10^{37} \text{ erg s}^{-1}, 1.0 \text{ cm}^{-3}$

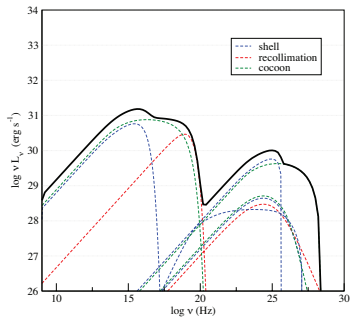


$10^5 \text{ yr}, 10^{37} \text{ erg s}^{-1}, 0.1 \text{ cm}^{-3}$



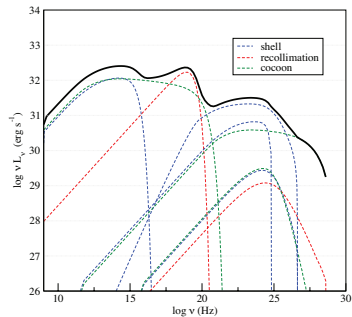
$10^5 \text{ yr}, 10^{37} \text{ erg s}^{-1}, 1.0 \text{ cm}^{-3}$

Broadband non-thermal emission



$10^{36} \text{ erg s}^{-1}$, 0.1 cm^{-3} , 10^4 yr , $d = 3 \text{ kpc}$

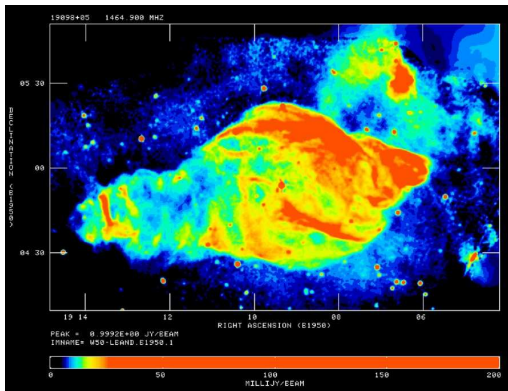
- $F_{5 \text{ GHz}} \sim 4 \text{ mJy}$
- $F_{0.1-10 \text{ keV}} \sim 7.3 \times 10^{-15} \text{ erg cm}^{-2} \text{ s}^{-1}$
- $F_{10-100 \text{ keV}} \sim 2.1 \times 10^{-15} \text{ erg cm}^{-2} \text{ s}^{-1}$
- $F_{100 \text{ MeV} \leq E \leq 100 \text{ GeV}} \sim 1.7 \times 10^{-16} \text{ erg cm}^{-2} \text{ s}^{-1}$
- $F_{>100 \text{ GeV}} \sim 2.8 \times 10^{-17} \text{ erg cm}^{-2} \text{ s}^{-1}$



$10^{37} \text{ erg s}^{-1}$, 1.0 cm^{-3} , 10^5 y , $d = 3 \text{ kpc}$

- $F_{5 \text{ GHz}} \sim 580 \text{ mJy}$
- $F_{0.1-10 \text{ keV}} \sim 1.4 \times 10^{-13} \text{ erg cm}^{-2} \text{ s}^{-1}$
- $F_{10-100 \text{ keV}} \sim 1.0 \times 10^{-13} \text{ erg cm}^{-2} \text{ s}^{-1}$
- $F_{100 \text{ MeV} \leq E \leq 100 \text{ GeV}} \sim 2.7 \times 10^{-14} \text{ erg cm}^{-2} \text{ s}^{-1}$
- $F_{>100 \text{ GeV}} \sim 1.5 \times 10^{-15} \text{ erg cm}^{-2} \text{ s}^{-1}$

Application to SS433/W50



(Dubner et al. 1998)

Application to SS433/W50

Source description

- First stellar compact object where relativistic jets were found (Spencer 1979)
- Binary system: $\sim 9 M_{\odot}$ black-hole and a $\sim 30 \pm 10 M_{\odot}$ A3–7 supergiant companion
- Distance ≈ 5.5 kpc
- P of 13.1 d in a \sim circular orbit, $i \approx 78^{\circ}$
- Precessing jets ($v_{\text{jet}} = 0.26 c$, $P_{\text{pr}} \sim 162$ d, $\theta_{\text{pr}} \sim 21^{\circ}$)
- Doppler shifted iron lines observed up to 10^{17} cm \Rightarrow in-situ reheating?
- Super-Eddington accretion disk, $M_{\text{accr}} = 10^{-4} M_{\odot}/\text{y}$
- Interaction with the surrounding W50 nebula ($\Rightarrow L_{\text{jet,kin}} \sim 10^{39}$ erg s $^{-1}$)
- Non-thermal radio-to-X-ray hot-spot emission both in the East and West “ears”

Observations of SS433 at VHE gamma-rays

Previous observations

- HEGRA observations in 1998–2001, for $t_{obs} \geq 100$ h (Aharonian et al. 2005)

Source	Obs. time [h]	$^a E_{th}$ [TeV]	θ_{cut} [deg]	s	b	$^b S$	$^c \phi_{crab}^{99\%}$ [σ]	$^d \phi^{99\%}$
— SS-433/W50 and associated —								
SS-433 <i>e1</i>	72.0	0.8	0.13	315	1972	-0.4	0.023	6.18
SS-433 <i>e2</i>	73.1	0.8	0.21	794	4980	-0.7	0.034	9.18
SS-433 <i>e3</i>	68.8	0.8	0.28	1247	8108	-2.0	0.032	8.96
SS-433	96.3	0.8	0.15	433	2541	+0.8	0.032	8.93
SS-433 <i>w1</i>	104.9	0.7	0.14	352	2168	-0.1	0.024	6.65
SS-433 <i>w2</i>	100.7	0.7	0.14	334	1994	+0.4	0.031	9.00

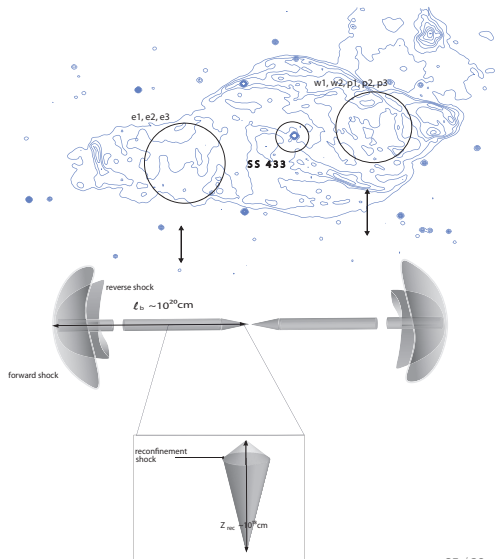
- CANGAROO-II observations in 2001–2002 of the western interaction region for $t_{obs} \sim 85$ h (Hayashi et al. 2009, astro-ph 0909.0133)

Source	R.A.	Decl.	$^a N_s$	$^b S$	$^c \phi^{99\%}$
<i>p1</i>	19 ^h 10 ^m 17 ^s	+4°57'46''	39	0.39	1.5
<i>p2</i>	19 ^h 09 ^m 44 ^s	+4°58'48''	-12	-0.11	1.3
<i>p3</i>	19 ^h 09 ^m 12 ^s	+4°59'13''	-97	-1.0	0.79

Jet-medium interaction model

Interaction model applied

Parameter	Value
Jet kinetic power Q_{jet} (erg s^{-1})	10^{39}
ISM density n_{ISM} (cm^{-3})	1
Source age t_{MQ} (yr)	5×10^4
Jet Lorentz factor Γ_{jet}	1.04
Jet opening angle Ψ ($^\circ$)	1.2
Star Luminosity L_\star (erg s^{-1})	10^{39}
Self-Similar parameter \mathcal{R}	3
Non-thermal fraction χ	0.01



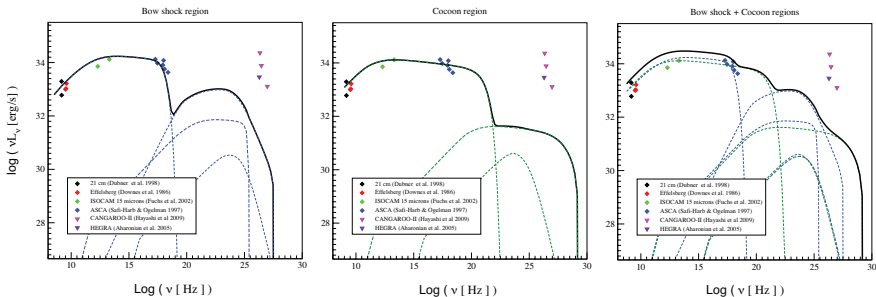
SS433/W50 interaction

- Bow shock at $\sim 6 \times 10^{20}$ cm
- Reverse shock at $\sim 4.5 \times 10^{20}$ cm
- Cocoon's width $\sim 5 \times 10^{19}$ cm

<i>Physical properties</i>	Inferred values
<i>SHELL</i>	
Magnetic field B (G)	6×10^{-5}
Shock velocity v_b (cm s^{-1})	4.4×10^7
Emitter size r (cm)	2.3×10^{20}
Rad. energy dens. u_* (erg cm^{-3})	5.0×10^{-14}
Maximum energy E_{max} (TeV)	54.2
Target density n_t (cm^{-3})	4.0

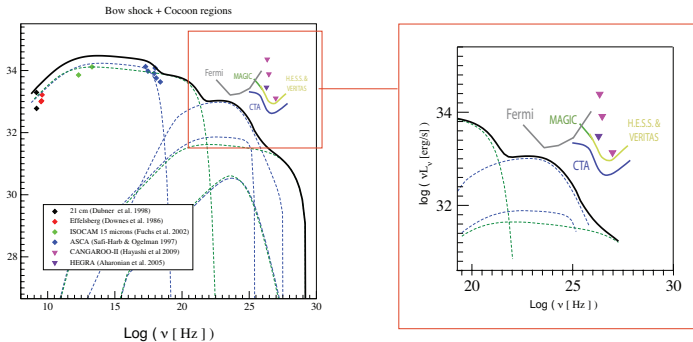
<i>Physical properties</i>	Inferred values
<i>COCOON</i>	
Magnetic field B (G)	3.8×10^{-5}
Shock velocity v_{BS} (cm s^{-1})	1.6×10^{10}
Emitter size r (cm)	5.5×10^{19}
Rad. energy dens. u_* (erg cm^{-3})	6.4×10^{-14}
Maximum energy E_{max} (TeV)	280.5
<i>RECONFINEMENT</i>	
Magnetic field B (G)	5.2×10^{-5}
Shock velocity v_{CONF} (cm s^{-1})	1.9×10^9
Emitter size r (cm)	1.9×10^{17}
Rad. energy dens. u_* (erg cm^{-3})	2.5×10^{-10}
Maximum energy E_{max} (TeV)	5.2

SS433/W50 interaction



- Radio: 1465 MHz eastern wing flux ~ 15 Jy \rightarrow (Downes et al. 1981; Dubner et al. 1998) $\Rightarrow \sim 10^{33}$ erg s $^{-1}$ ($d = 5.5$ kpc) \approx predicted by the model.
- X-rays: $L_{0.4-4.5 \text{ keV}} \sim 10^{34}$ erg s $^{-1}$ (Safi-Harb & Petre 1999) \sim X-ray flux from both the bow shock and cocoon (although it extends to higher energies in this case)

SS433/W50 interaction



- γ -rays: $E \geq 100 \text{ GeV} = 2.27 \times 10^{-14} \text{ ph cm}^{-2} \text{ s}^{-1} \ll$ current Cherenkov sensitivities < next CTA sensitivities ?

Conclusions

- Extragalactic interaction model easily applied to μ -quasars
- hydrodynamical simulations \rightarrow pressures, mass densities and source geometry: good agreement with analytical model
- Multiple conical shocks present in hydrodynamical simulations, vs one only shock in the analytical model
- Radio to X-ray fluxes could be detected, gamma-ray fluxes too faint (see however Zhang & Feng 2010)
- Dependence on the ambient density profile not accounted for
- pp interactions not studied (e.g., Heinz & Sunyaev 2002)
- SS 433/W50: strong candidate (high L_{jet} , high n_{ISM} in the W50 nebula)
- interactions remain undetected at VHE γ -rays (HEGRA & CANGAROO-II): target for next generation IACTs?)

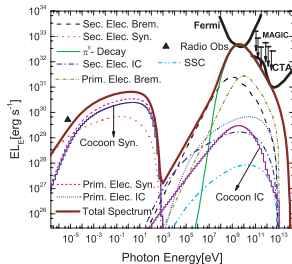
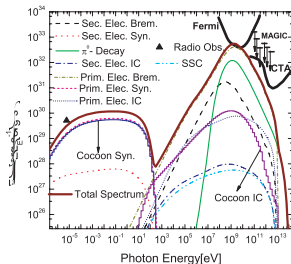
Zhang & Feng (2010):

"Non-thermal emission from the termination of microquasar jets"

Application to Cyg X-1

Table 2. Parameters adopted to calculate SEDs.

Parameter	Fig. 2	Fig. 3	Fig. 4
Ratio of L_{jet} to L_{non}	0.01	0.1	0.1
Source age t_4 (10^4 yr)	3	3	3
L_{39} (10^{39} erg s^{-1}) ^a	1	1	1
Power-law index	1.8	2	1.8
Temperature T_4 (10^4 K) ^b	3	3	3
Diffusion radius R (pc)	3.5	3	3
Magnetic field B (μ G)	12	6	5.5
Ratio of L_c to L_p (K_{cb})	0.01	1	1
Shell width r_{sh} (pc)	0.8	0.6	0.7
Shell density n_{H} (cm^{-3})	250	1000	900
Shell length l_{sh} (pc)	10	9	11

^aIndicates the luminosity of stellar companion.^bThe stellar effective surface temperature.**Figure 2.****Figure 3.****Figure 4.**